Available online at www.sciencedirect.com
SCIENCE DIRECT®
Electrochimica Acta 50 (2005) 1413–1422
ELECTROCHIMICA Acta
www.elsevier.com/locate/electacta

Variations in interfacial properties during cell conditioning and influence of heat-treatment of ionomer on the characteristics of direct methanol fuel cells

Fuqiang Liu, Chao-Yang Wang*

Department of Material Science and Engineering, Electrochemical Engine Center, Pennsylvania State University, University Park, PA 16802, USA

Received 21 May 2004; received in revised form 21 August 2004; accepted 21 August 2004
Available online 8 October 2004

Abstract

Variations in interfacial properties in the anode catalyst layer during cell conditioning were characterized, and influence of the heat-treatment of ionomer on the characteristics of direct methanol fuel cells was investigated in this work. The anode catalyst layer was made by mixing a solvent-substituted Nafion solution with unsupported Pt/Ru black and curing the mixture in an oven with an inert environment. Materials characterization (SEM and optical microscopy) and electrochemical characterization (cell polarization, anode polarization, electrochemical impedance spectroscopy, and CO-stripping cyclic voltammetry) were performed. During cell conditioning, the enhanced kinetics of MeOH electrochemical oxidation and severe limiting current phenomenon are due to the combination of variations in interfacial properties and swelling of ionomer in the anode catalyst layer over time. Ru oxides at the catalyst surface are reduced continuously during cell conditioning. The nearly constant integrated areas under the CO-stripping CV peaks and broadened peak shapes indicate a stable number of Pt/Ru bimetallic alloy surface sites, yet the surface composition distribution is broadened. Heat-treatment influences ionomer crystallinity, altering its swelling behavior and hence affecting the characteristics of the direct methanol fuel cell (DMFC) anode.

Keywords: Direct methanol fuel cells; Catalyst layer; Nafion; Interfacial properties; Conditioning

1. Introduction

Direct methanol fuel cells (DMFCs) are receiving more and more attention for their potential as new-generation, portable power sources. The membrane electrode assembly (MEA) is the heart of a DMFC, and consists of cathode gas diffusion layer (GDL), cathode catalyst layer, anode GDL and anode catalyst layer, in addition to a polymer electrolyte membrane. The performance of DMFCs is strongly affected by the electrode/MEA structure as well as its preparation techniques, making these key issues in the development of DMFCs [1].

The catalyst layer, where the electrochemical reaction takes place, must fulfill three functions: proton conduction, electron conduction and reactant access [2]. The main requirement of a good electrode is the maximized catalyst/ionomer/reactant interface or triple-phase boundary. Ordinarily, the catalyst/ionomer interface is formed by impregnating or directly mixing catalyst powders with an ionomeric polymer (usually Nafion) before hotpressing the electrode onto the membrane, to maximize contact of catalyst particles with the ionomer. It is understood that the presence of ultra thin ionomer films covering the catalyst particles is important for constructing highly active electrodes.

Wilson and co-worker at Los Alamos developed a method in which the catalyst and Nafion were mixed together, and the resultant catalyst ink was applied to a PTFE decal and was

* Corresponding author. Tel.: +1 814 863 4762; fax: +1 814 863 4848.
E-mail address: cxw31@psu.edu (C.-Y. Wang).

0013-4686/$ – see front matter © 2004 Elsevier Ltd. All rights reserved.
doi:10.1016/j.electacta.2004.08.040

subsequently transferred onto a membrane, or directly coated on a membrane [3–7]. It is reported that this method provided better power density and cell internal resistance compared to the conventional method, due largely to an extended catalyst/ionomer interface and hence a dramatic improvement in catalyst utilization. Subsequently, as a preliminary step toward understanding the interaction of the ionomer and catalyst, Uchida et al. [8–10] reported that good cell performance can be obtained by using solvents with an intermediate dielectric constant of $3< \varepsilon <10$ (e.g. butyl acetate), which form a colloid of Nafion. This is due to increased interaction of Nafion and catalyst and extended reaction interface as compared to using high-dielectric-constant solvents such as water or alcohols. But others [11,12] reported that the electrode prepared using high dielectric-constant solvents could also produce superior performance over those made with lower dielectric constants. Aricò et al. [13] tried to use XRD, SEM, and TEM to investigate the Nafion/catalyst interface, but no interaction between catalyst and ionomer was detected and no significant interconnected network of Nafion micelles inside the catalyst layer was observed. To date, a basic understanding of the microstructural interface in electrodes and the influence of solvents is still incomplete.

One of the significant parameters affecting the cell performance is the ionomer-to-carbon (I/C) ratio. The influence of Nafion content on performance of fuel cells has been a subject of much investigation [14,15]. An I/C ratio of 30% is preferred to achieve minimum ionic resistance and maximum contact of ionomer with Pt particles [2]. Even maintaining this I/C ratio, cell performance of MEA fabricated using identical catalyst inks varies significantly for different methods. This may be due to variation in catalyst/ionomer interfaces formed using different fabrication procedures. Thus, in most cases it is difficult to definitively establish the impact of fabrication parameters, such as solvents and Nafion content, upon observed properties such as fuel cell performance and catalyst/ionomer interface.

Although extensive studies have sought to increase the catalyst/ionomer interface and to fabricate high-performance MEAs, due to the complex structure of the catalyst layer and MEA, the precise nature of catalyst/ionomer interface and the method of maximizing it are still unclear. This problem is further complicated by the fact that changes of interfacial properties and interfacial structure of catalyst/Nafion take place during the process of cell conditioning.

In this paper, variation of interfacial properties during cell conditioning and the influence of heat treatment of ionomer on the anode catalyst layer performance, methanol crossover and catalyst/ionomer interface were investigated. Anode polarization, CO-stripping cyclic voltammetry (CV) and electrochemical impedance spectroscopy (EIS) measurements were taken to probe the internal structural and interfacial variations during cell conditioning. It is hoped that the results obtained herein will contribute to the understanding of the structure of the catalyst layer and particularly the ionomer/catalyst interface.

2. Experimental

2.1. MEA fabrication

Pretreatment of the Nafion 112 membrane, preparation of MEAs, and the single-cell hardware have been detailed in previous publications [16,17]. A brief description is given here.

Both anode and cathode backing layers were 20% FEP wet-proofed carbon paper (Toray TGPH-090, E-TEK) of 0.26 mm in thickness. A mixture of Vulcan XC72R carbon black and 40% dry weight TEFLON emulsion (TFE 30, Dupont) was coated on the carbon paper using a gap-adjustable doctor blade to form a microporous layer. Subsequently, the coated carbon paper was dried in an oven at 100 °C for 30 min and then at 360 °C for 15 min. Carbon and PTFE loadings of the microporous layer were controlled at 2 mg/cm^2.

A commercial 5 wt.% Nafion solution (EW 1100, Aldrich) was modified by addition of diluted sodium hydroxide solution and a viscous organic solvent (e.g. ethylene glycol) to make solvent-substituted Nafion solution. This Nafion solution was mixed with unsupported Pt/Ru black (HiSPEC 6000, Pt:Ru = 1:1 atomic ratio, Alfa Aesar) in a nitrogen-protected environment. The resultant slurry was coated on the microporous layer using the doctor blade to form the anode catalyst layer. The loadings of Pt/Ru and Nafion in the anode catalyst layer were controled at 5 and 1.2 mg/cm^2, respectively. The cathode was made by the same method. The 40 wt.% Pt/C (E-TEK) was used and the loadings of Pt and Nafion in the cathode catalyst layer were about 1.3 and 1 mg/cm^2, respectively. After the catalyst slurries were coated onto the microporous layer, the anode and cathode were cured at 160 °C in a nitrogen-filled vacuum oven. By this solution cast and post-heat-treatment process, the ionomer (Nafion) in the catalyst layer forms a durable and insoluble film around the catalyst particles, resulting in a more robust MEA. After being re-protonated to hydrogen form of Nafion by using 0.1 M sulfuric acid solution, the anode and cathode were hotpressed to a pretreated Nafion 112 membrane at 125 °C and 100 kgf/cm^2 for 3 min.

2.2. Micro-structural analysis

Scanning electron microscopy (SEM, Philips 420 ST) was used to analyze the thickness and surface of the anode catalyst layer. In order to observe the change in surface morphology before and after wetting the Pt/Ru catalyst layer with MeOH solution, a high-resolution 3-CCD video camera (Sony DCR VX2000) was used instead. After the anode catalyst layer was fully hydrated in 2 M MeOH solution,

the surface was analyzed by the high-resolution CCD camera quickly to prevent dehydration of ionomer in the anode catalyst.

2.3. Electrochemical studies

After the MEA was installed in the cell, 2 M MeOH solution was fed into the anode inlet at flow rate of 3 ml/min by a peristaltic pump without pre-heating and back pressure, after which the cell temperature was increased. The conditioning time was counted after the desirable cell temperature was reached.

To investigate the interfacial property changes during cell conditioning, electrochemical characterization, including EIS and CO stripping CV, was conducted at room temperature (25 °C) using a Solartron 1278 electrochemical interface in conjunction with a Solartron 1260 frequency response analyzer. In EIS experiments, the working electrode was linked to the Pt/Ru anode side, fed with humidified nitrogen, and the reference and counter electrodes were connected to the Pt cathode side, which was fed with humidified hydrogen. The flow rates of H_2 and N_2 were approximately 100 ml/min. EIS spectra were obtained by applying a 10 mV sine wave in the frequency range of 0.1 Hz to 10 kHz. CO-stripping CVs of the Pt/Ru anode catalysts was carried out at room temperature using a 5-cm^2 graphite cell, with N_2, or CO plus N_2 fed to the anode serving as the working electrode. Humidified H_2 was fed to the Pt cathode at 100 ml/min and zero back pressure, which acted as a counter and pseudo-reference electrode (dynamic hydrogen electrode, DHE). Humidification temperatures of the N_2, or CO plus N_2 were 40 °C. CO was adsorbed onto the Pt/Ru catalyst surface by feeding 1000 ppm CO in N_2 at 500 ml/min (zero back pressure) through the anode for 30 min, while holding the Pt/Ru catalyst electrode potential at 0.1 V versus the DHE. The gas was then switched for 10 min to N_2 at the same flow rate, with the potential still held at 0.1 V to remove any CO from the gas phase. Then the potential was scanned from 0.1 to 0.85 V at 5 mV/s, to record the CO stripping CVs. The anode polarization curves were measured by feeding room-temperature humidified H_2 to the cathode side as the preudo-reference electrode, with respect to which the voltage was applied.

To investigate the influence of heat-treatment of ionomer in the anode catalyst layer on DMFC performance, non-humidified, 15 psi room-temperature air was fed into a cathode inlet at a flow rate of about 600 ml/min when the cell polarization curves were measured. After each scan, the MEA was soaked with static MeOH solution at 80 °C without airflow or load to fully hydrate the polymer membrane. MeOH crossover and anode polarization curves were measured by feeding humidified N_2 and H_2 into cathode inlet, respectively. Cell performance, MeOH crossover and anode polarization curves were obtained by using an Arbin BT +4 testing system in a galvanodynamic polarization mode with a scan rate of 3 mA/s.

3. Results and discussion

3.1. Variations in interfacial properties of the anode during cell conditioning

For all results to be presented in this section, the catalyst-coated anode used was cured at 160 °C in a nitrogen-filled vacuum oven for 40 min. The cathode remained in the oven overnight.

3.1.1. SEM and optical micrograph

Fig. 1a and b show SEM micrographs of the cross-section and surface of the anode catalyst layer. Fig. 1a shows a planar microporous layer with an average thickness of 30 μm over a carbon paper backing. On top of the microporous layer, an anode catalyst layer of about 20 μm in thickness consisting of unsupported Pt/Ru black and Nafion polymer is observed to be more porous than the micropurous layer. Fig. 1b displays the microstructure of the anode catalyst layer in high magnification. The diameter of the agglomerates formed by Pt/Ru black and Nafion, is found to be from several μm to about 10 μm. Some small pores in the agglomerates can be

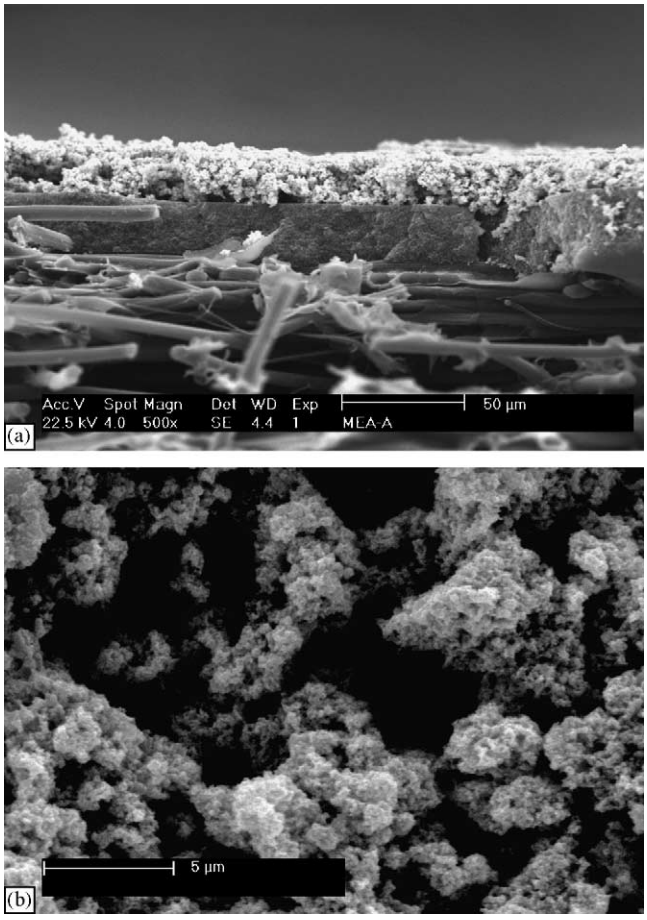

Fig. 1. SEM micrographs of: (a) cross-section and (b) surface of anode catalyst layer. The electrode was cured at 160 °C in a nitrogen-filled vacuum oven for 40 min. Unsupported Pt/Ru was used as the anode catalyst.

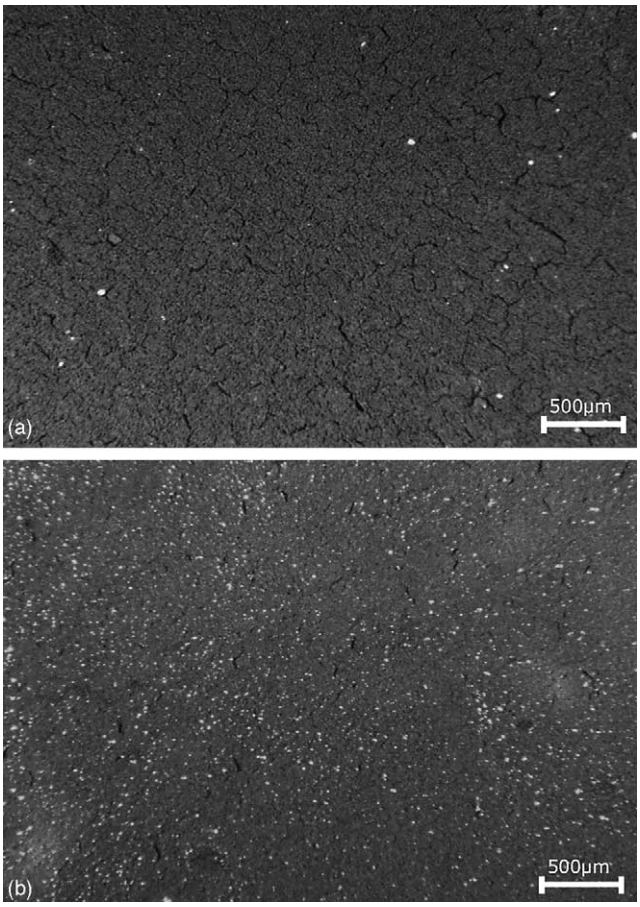

Fig. 2. Optical micrographs of anode catalyst surface: (a) dry state and (b) fully-hydrated state by 2 M MeOH solution at room temperature.

observed in diameter smaller than 1 μm. Watanabe et al. [18] had characterized the microstructure of a gas-diffusion electrode, reporting that the catalyst layer had two distinctive pore-size distributions with a boundary at ca. 0.1 μm. The small pores (primary pores) were identified within primary particles forming agglomerates, and the larger pores (secondary pores) were between the agglomerates. The results of the present study are consistent with those reported, with the diameter of the secondary pores in the range of about 5–6 μm.

Fig. 2a and b show optical micrographs of the surface of the anode catalyst layer before and after being fully hydrated by 2 M MeOH solution. In Fig. 2a, large pores and uniform cracks (mud cracking), introduced into the catalyst layer due to volume shrinkage of the catalyst slurry during annealing, can be observed. In the fully hydrated state, however, as shown in Fig. 2b, some of these pores and cracks disappear, due to the swelling and expansion of Nafion ionomer after full hydration. In operation of DMFCs, the anode catalyst layer remains in contact with MeOH solution, so the Nafion ionomer in the catalyst layer expands and thus the porosity in the catalyst layer is reduced. Its influence on DMFC performance will be discussed in the next subsection.

3.1.2. Electrochemical characterization of anode during cell conditioning

Before use in fuel cells, MEAs require a conditioning process to obtain repeatable performance. The conditioning process is accompanied by the time-dependant swelling behavior of ionomer and interfacial property variations in the catalyst layer.

This experiment recorded anode polarization measurements after the exposure to 2M MeOH solution at room temperature. CO-stripping CVs and EIS were measured sequentially at various points in time during this conditioning process. The results of EIS, anode polarization curves, and CO-stripping CVs measured over time are shown in Figs. 3–5.

Fig. 3a and b show the EIS spectra and internal cell resistance variations (intersects of EIS spectra with the real axis) measured over time during cell conditioning, respectively. The internal resistance initially dropped dramatically, from 0.322 Ω cm^2 at 30 min, to 0.246 Ω cm^2 at 568 min. Beyond 568 min the curve begins to level off, indicating a negligibly small variation with time or attainment of steady state.

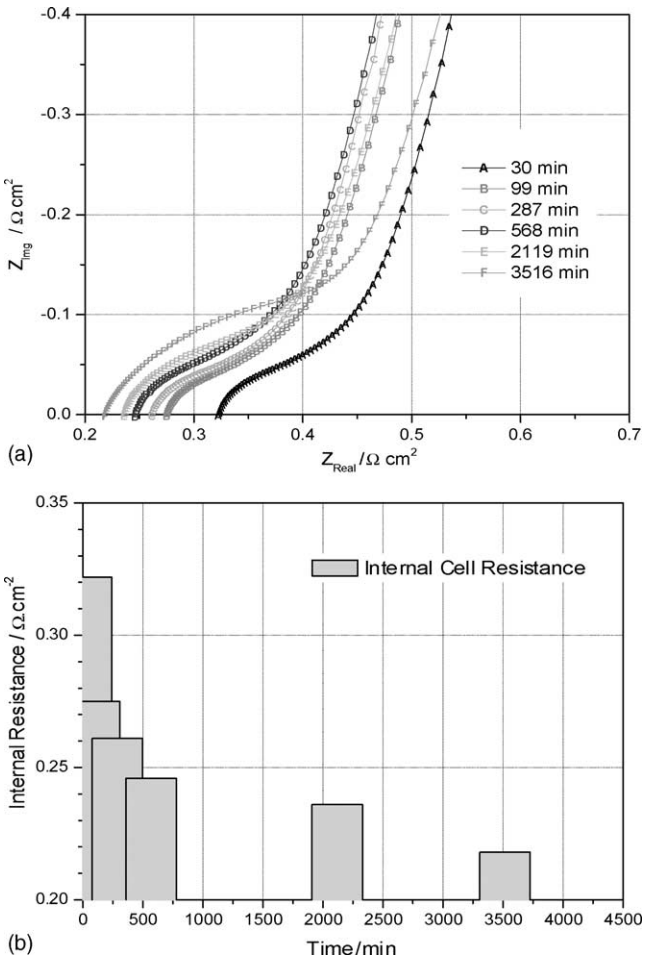

Fig. 3. (a) Nyquist plots as a function of conditioning time and (b) internal cell resistance versus conditioning time. The cell was operated under 25 °C, using humidified H_2/N_2 at cathode and anode, respectively. The frequency range was from 100 kHz to 0.1 Hz.

It is indicated by Boyer et al. [19] that the specific proton conductivity of a catalyst layer prepared with recast Nafion is proportional to the volume fraction of Nafion in the catalyst layer. Saab et al. [20] reported that when swelled by water vapor, the ionic resistance in the catalyst layer decreased, while the electronic resistance increased. In the process of conditioning, the Nafion ionomer in the catalyst layer continues swelling with time until steady state is reached, therefore the effective ionic and electronic conductivities in the catalyst layer vary: the ionic resistance decreases, while the electronic resistance increases with time. In the present experiment, the diameter of the high-frequency semi circles expanded with time, a trend unlike that reported in the literature where at high frequencies, a Warburg-like region (45° slope) corresponding to ion migration through the catalyst layer became smaller as the ionic resistance decreased [2,21,22]. These contrasting results may result from some unexpected interfacial property changes occurring during MeOH conditioning or different electrode structures we used.

Fig. 4 shows anode IR-corrected polarization curves as a function of conditioning time after correcting the cell ohmic drop. The anode potentials shift significantly to lower values over time; however, at 2119 and 3516 min, the anode voltages continue shifting to lower values at low current density region (<60 mA/cm^2). Beyond 60 mA/cm^2, however, the voltages curve upward very steeply, exceeding previous values. The curves beyond 3516 min remains largely unchanged with time, and are not plotted here.

Fig. 5 shows the CO stripping CV curves measured over time during cell conditioning with methanol, indicating a trend of significant peak broadening and negative shifting to lower cell voltage. For example, the peak potential shifts to 0.4355 V versus DHE after about 3516 min compared to 0.4706 V initially. Interestingly, the integrated areas under the peak do not change with conditioning time within the experimental error. Ha et al. [23] observed similar phenomenon when using H_2 and methanol to condition formic acid fuel cells: the methanol-conditioned anode showed a CO-stripping peak broadening and negative shifting compared with the H_2-conditioned anode.

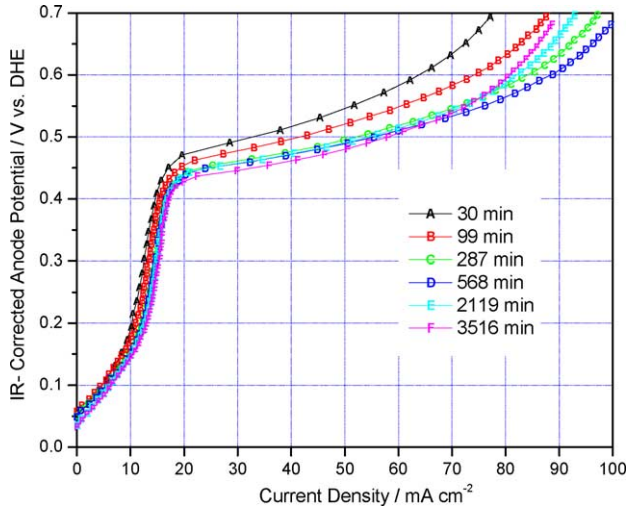

Fig. 4. IR-corrected anode polarization curves recorded over time during cell conditioning. The experiment was operated at 25 °C, using 2 M MeOH and 3 mA/s scanning rate.

CO-stripping peak potential can be correlated to Ru surface content, and can be used as an in-situ tool to probe the Pt/Ru anode surface composition [24]. According to the calibration curve [24] at the same temperature (25 °C) and scan rate (5 mV/s), the potentials of 0.4706 and 0.4355 V (Fig. 5) observed at 30 and 3516 min correspond to Pt/Ru metal alloy with Ru surface content of ∼15 and 45%, respectively. Note here that the average bulk composition of the as-received catalyst is Ru:Pt = 50:50. It is thus shown that Ru oxides at the catalyst surface can be reduced continuously during cell conditioning. The near constant integrated areas under the CO-stripping peaks and broadened peak shapes indicate a stable number of Pt/Ru bimetallic alloy surface sites, yet the surface composition distribution is broadened. It appears that reduction of Ru oxides and possible subsequent Pt/Ru alloying occur in the DMFC anode during cell conditioning.

Combining the data shown in Figs. 4 and 5, the variation in anode polarization curves during cell conditioning can be explained by the surface composition change of the Pt/Ru catalyst. Surface Ru enrichment can enhance the kinetics of methanol oxidation, as indicated by the negative shift of the peak potential and onset potential of CO-stripping CVs. When the potential scans beyond the peak potential, however, metal oxides [25] or weakly absorbed intermediates [26] form on the Pt/Ru surface to prevent further reaction of methanol, causing the abrupt increase of anode potential at higher current density region or what is known as the limiting current. The porosity loss in the anode catalyst layer caused by Nafion swelling can also cause the mass transport limiting current, as will be elaborated in the next section.

3.2. Influence of heat-treatment of ionomer on the anode

To investigate the influence of heat-treatment of ionomer in the anode catalyst layer on the cell characteristics, two different MEAs, MEA-1 and MEA-2, were prepared. Anodes of MEA-1 and MEA-2 were cured in vacuum for 40 and 60 min, respectively. The cathodes of the two MEAs were identical and were treated in the oven overnight.

3.2.1. Performance variation in two different MEAs during conditioning

Variations of performance over time for the two MEAs are plotted in Fig. 6. The first scans of the two MEAs (at third min for MEA-1, fourth min for MEA-2) are almost identical. With time, however, the performance of MEA-1 improved and finally developed a very apparent limiting current phenomenon. For MEA-2, the changes are not so apparent, with no identifiable limiting current phenomenon. Beyond 1386 and 1225 min for MEA-1 and MEA-2, respectively, the performance of the two MEAs remained un-

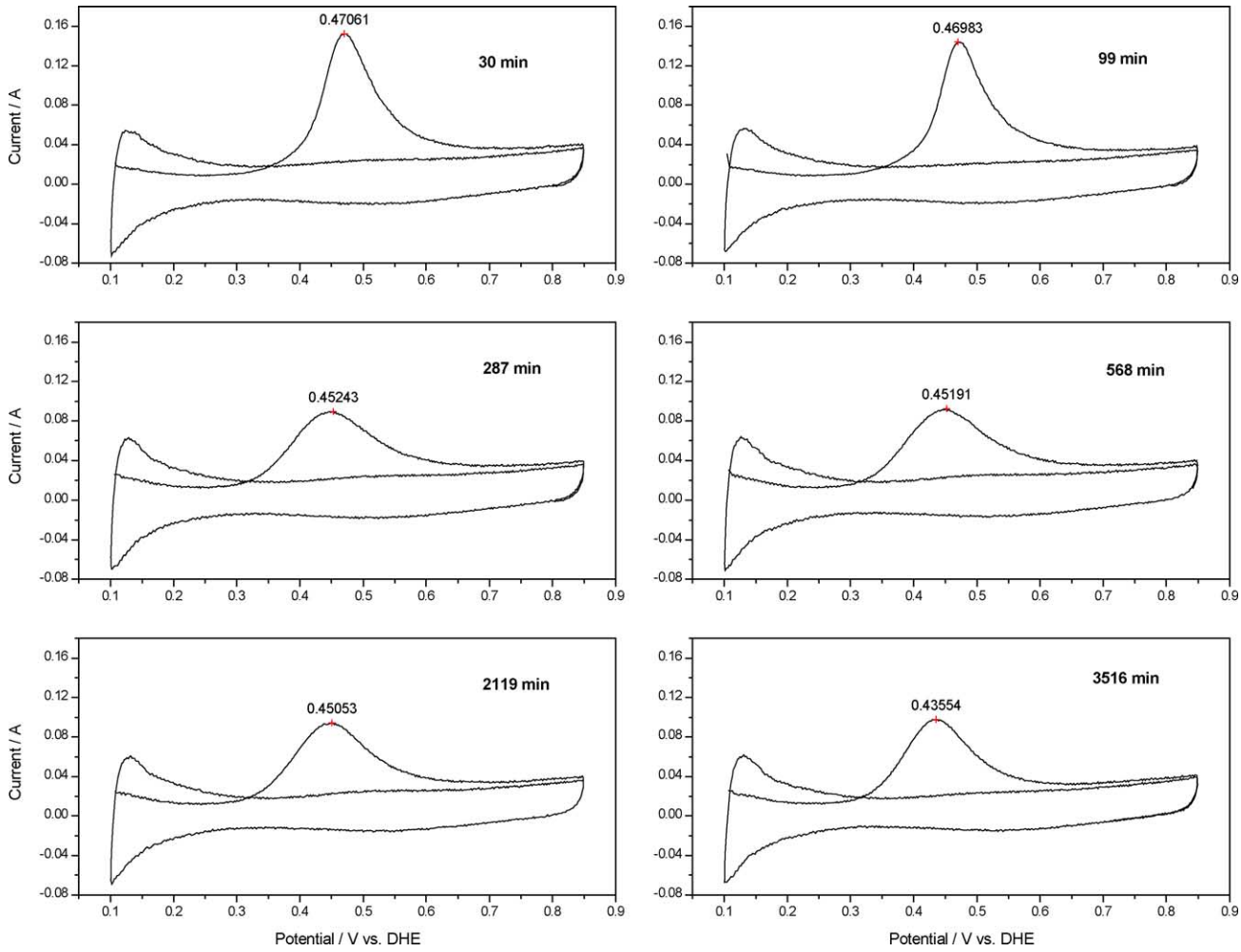

Fig. 5. CO stripping CVs curves measured over time during cell conditioning using methanol at scan of 5 mV/s, in N_2 environment.

changed with time and can maintain stable performance for days. Performance beyond these time limits can be considered as stable and therefore no polarization curves are plotted here.

Fig. 7 shows the plots of current densities over time at the cell voltages of 0.45, 0.4, 0.3, 0.25, and 0.2 V. In the first 100 min, the current densities increase dramatically over time, with MEA-1 changing faster. Beyond 500 min, the current densities for MEA-2 at higher cell voltages remain unchanged with time, and the current densities at lower cell voltages increased somewhat. On the contrary, for MEA-1, the current density at 0.3 V cell voltage remains almost unchanged with time beyond 100 min during conditioning. What is most interesting is that the current density variations with time at higher cell voltages of 0.4 and 0.45 V show different trends than those at lower cell voltages of 0.2 and 0.25 V. At lower cell voltages, the current densities continue to increase throughout conditioning, while at higher cell voltages, the current densities first increased very quickly followed by a plateau, and then decreased. For example, the current density at 0.2 V cell voltage increased from 470 mA/cm^2 at 3 min to 700 mA/cm^2 at 636 min and then dropped down to less than 600 mA/cm^2 at 1375 min. The limiting current density of MEA-1 after conditioning is only slightly above 600 mA/cm^2.

Besides the surface properties of catalysts, limiting current phenomenon may be caused by mass transport limitation of reactant or proton migration through the ionomer in the electrode. Proton migration cannot provide a reasonable explanation for the limiting current phenomenon observed in this experiment. The anode backing and micro porous layer (MPL) can serve as a methanol barrier [16,17,27], but in this case, they cannot explain the increasingly severe limiting current phenomenon over time using the same anode backing and MPL. As discussed above, the limiting current may be caused by a combination of surface Ru enrichment and decrease of porosity in the catalyst layer. The influence of surface Ru oxide reduction on anode polarization has been discussed previously, thus only the influence of the hydration of ionomer is considered here.

Dry Nafion membranes are composed of ionic clusters dispersed in a perfluorinated matrix which are fused together in the catalyst layer fabrication. The swelling behavior of these polymers is very sensitive to external conditions, such as tem-

perature, relative humidity, equilibrating solution, and heat treatment history [28]. In these membranes, phase separation between the hydrophobic fluorocarbon backbone and the hydrophilic sulfonic acid groups occurs. Nafion recast at low temperature has very low crystallinity, resulting in high solubility and inferior mechanical properties [29–32], but with annealing of the solution-recast films at high temperature, the fluorocarbon chains in the polymer film can again fuse together to form a durable and insoluble layer [29,30,33]. The size of the clusters formed by ions and water molecules in the anode catalyst layer tends to increase when contacting methanol solution, but the extent of growth is limited by the covalent bonds between these clusters and crystalline fluorocarbons. Extended or high-temperature heat treatment can increase the crystallinity of fluorocarbon, reducing the swelling of ionic clusters of ionomer in catalyst layers. In this work, the ionomers in the anode catalyst layer were cured for a selected time of 40 and 60 min for MEA-1 and MEA-2, respectively. So the crystalline contents of the ionomers in the anode catalyst layers of the two MEAs are different:

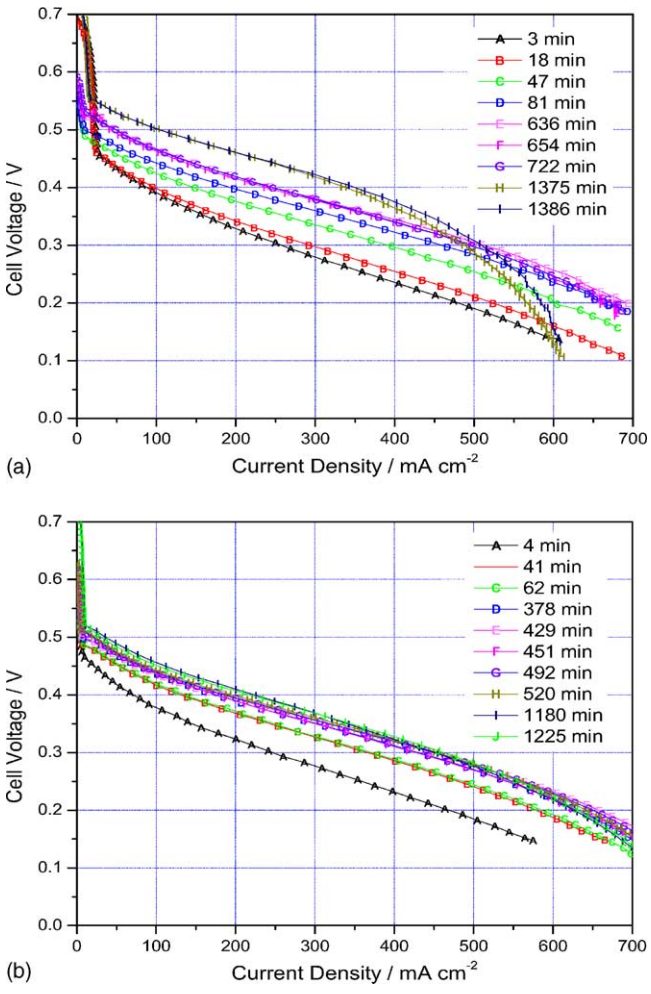

Fig. 6. Performance variation over time for two MEAs: (a) MEA-1 and (b) MEA-2.The cells were operated at 80°C, using 3 ml/min of 2 M MeOH solution and 15 psi, 600 ml/min dry air.

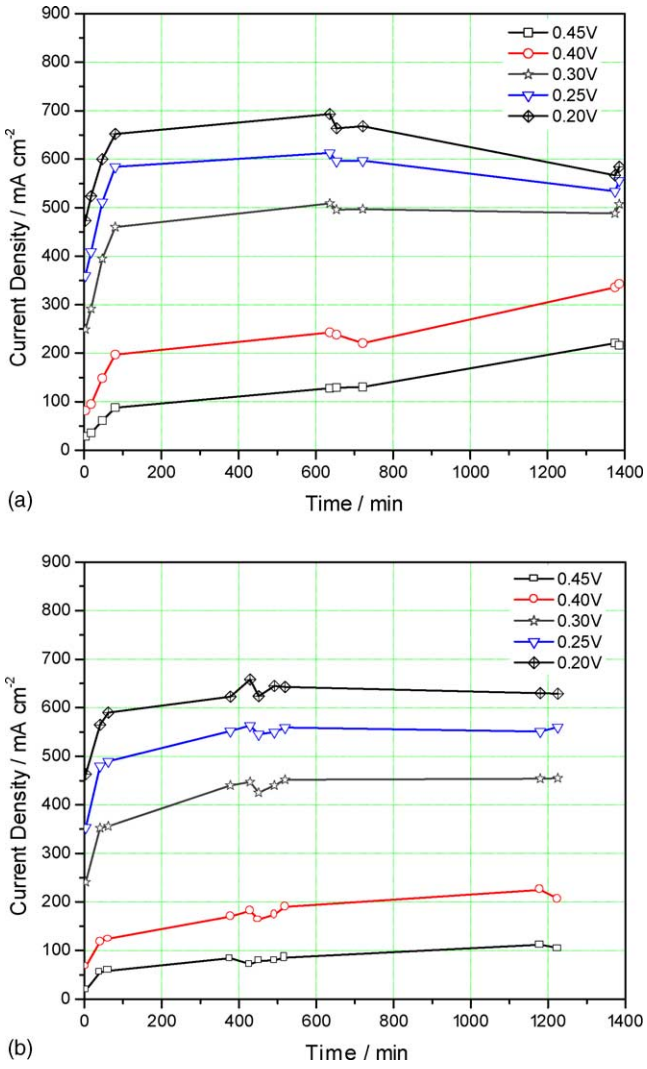

Fig. 7. Current densities at 0.45, 0.4, 0.3, 0.25, and 0.2 V cell voltages over time for two MEAs: (a) MEA-1 and (b) MEA-2. The cells were operated at 80 °C, using 3 ml/min of 2 M MeOH solution and 15 psi, 600 ml/min dry air.

the 60-min-treated anode had higher crystallinity than that with the 40-min-treated. Thus, for MEA-2 the ionomer in the anode catalyst layer could not swell appreciably, while for MEA-1, a larger degree of swelling due to low crystallinity was evident.

When contacting methanol solution, the anode catalyst layer would swell with time, but as the volume increases of the catalyst layer are limited by the anode backing, GDL and polymer electrolyte membrane on both sides, it tends to compress itself and possibly reduce the pore size and porosity. The anode catalyst layer of MEA-1 is much denser than that of MEA-2. Limiting current phenomenon of MEA-1 is attributed to a very dense anode structure. These experimental results indicate that in addition to anode backing and MPL, the anode catalyst layer can also act as a methanol barrier.

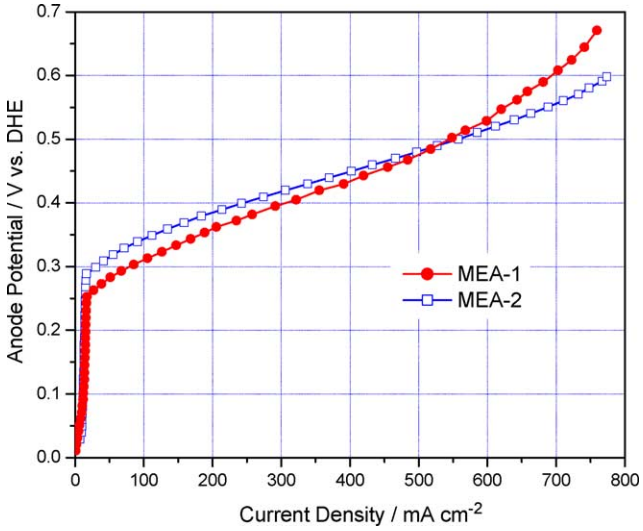

Fig. 8. Anode polarization curves of two MEAs after conditioning. The cells were operated at 80 °C, using 3 ml/min of 2 M MeOH solution and 15 psi, 100 ml/min humidified H_2.

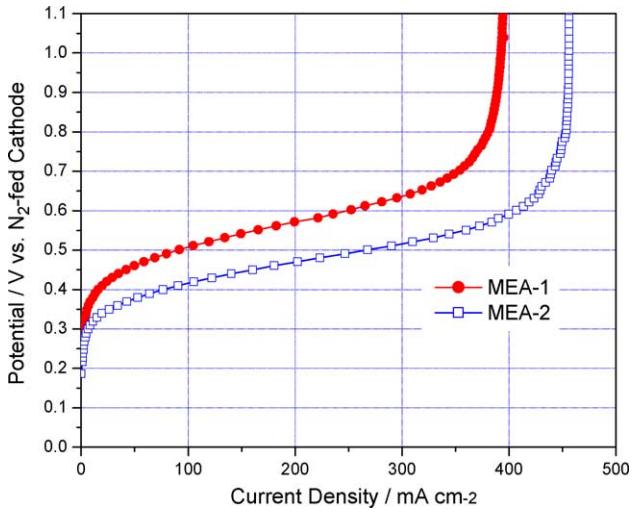

Fig. 9. MeOH crossover results of two MEAs after conditioning. The cells were operated at 80 °C, using 3 ml/min of 2 M MeOH solution at anode side and 15 psi, 100 ml/min room-temperature humidified N_2 at cathode side.

3.2.2. Anode polarization and MeOH crossover measurements

Fig. 8 presents the anode polarization curves of the two MEAs after conditioning. The anode of MEA-1 performs better than that of MEA-2 at current density below ca. 550 mA/cm^2, but at higher current density, the potential versus DHE increases dramatically. Beyond current density of 550 mA/cm^2, the anode of MEA-1 showed considerably more severe limiting current phenomena. Uchida et al. [8] found that increasing the amount of Nafion increases the catalyst coverage, fills the pores and decreases the pore volume, since the polymer penetrates only into the secondary pores between the agglomerates of catalyst particles. As discussed earlier, the ionomer in MEA-1 swelled more than MEA-2, causing the secondary pores to be reduced and hence a lower mass-transport limiting current.

Fig. 9 displays the MeOH crossover measurements of the two MEAs after conditioning. The oxidation current increases with the potential applied at the cathode side fed with room-temperature humidified N_2, until a limiting current occurs. The limiting current corresponds to the oxidation current of all the cross-over MeOH from the anode to cathode. The methanol crossover current densities of MEA-1 and MEA-2 are 395 and 455 mA/cm^2, respectively. MEA-1 shows a smaller MeOH crossover current than MEA-2, which can be explained by the denser anode structure of more swollen MEA-1.

The polarization curves and power densities of the two MEAs after conditioning are compared in Fig. 10. At 0.4 V, MEA-1 reaches a current density of 350 mA/cm^2, corresponding to 140 mW/cm^2; while MEA-2 produces only 225 mA/cm^2 and power density of 90 mW/cm^2 at the same cell voltage. By comparing Figs. 8 and 10, the slight superior anode polarization behavior of MEA-1 over MEA-2 probably cannot explain the large performance difference between the two MEAs, assuming that the cathodes of the two MEAs behave identically. Instead, this can be explained by the larger MeOH crossover of MEA-2, since at lower current densities (higher cell voltage), there is a large amount of MeOH crossover from the anode to cathode.

The methanol crossover current density can be mathematically formulated by a simple relation between the crossover current, I_{xover}, and the anode mass-transport limiting current density, $I_{\text{A,lim}}$ [34]. That is:

$$I_{\text{xover}} = I_{\text{xover,oc}} \left(1 - \frac{I}{I_{\text{A,lim}}}\right) \quad (1)$$

where $I_{\text{xover,oc}}$ is the crossover current density at open circuit, and I the operating current density. The anode limiting current density of MEA-1 is about 610 mA/cm^2, while that of MEA-2 is not so well defined, having an approxi-

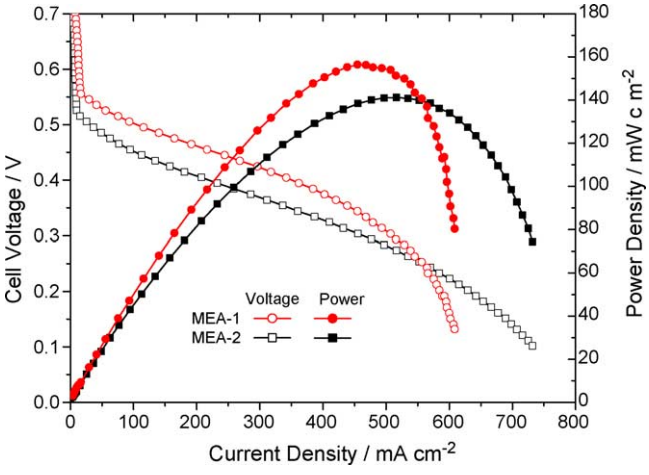

Fig. 10. Polarization and power density curves for two MEAs after conditioning. The cells were operated at 80 °C, using 3 ml/min of 2 M MeOH solution at anode and 15 psi dry air at cathode.

mate value of 750 mA/cm^2. According to Eq. (1) and using the methanol crossover rate at open circuit in Fig. 9, the crossover current densities at 0.4 V for the two MEAs are 168 and 319 mA/cm^2, respectively. The methanol crossover current of MEA-2 nearly doubles that of MEA-1. In DMFCs, the fuel efficiency due to methanol crossover is defined as:

$$\eta_{\text{fuel}} = \frac{I}{I + I_{\text{xover}}} \quad (2)$$

It follows that the fuel efficiency for MEA-1 reaches 68% compared with only 41% for MEA-2.

In this work, a thin Nafion membrane (Nafion 112, 50 μm) was used. A thin membrane reduces the cell internal resistance, but increases methanol crossover as well. The crossover methanol from the anode to cathode not only reduces fuel efficiency, but also deteriorates cathode performance. The larger methanol crossover is the major reason that causes the inferior performance of MEA-2 compared to MEA-1 at higher cell voltages. The performance of a DMFC is controlled by the anode polarization, cathode polarization and methanol crossover through the polymer electrolyte membrane. Thus, controlling the heat-treatment of ionomer in the anode catalyst layer provides a useful tool to optimize these factors in order to attain high DMFC performance, high fuel efficiency and thus high energy efficiency.

4. Conclusion

During cell conditioning, the Nafion ionomer in the catalyst layer expands and hence the pores in the catalyst layer shrink, leading to lower anode potential in the low current density region and development of severe limiting current. The internal resistance initially drops dramatically but eventually levels off, indicating that a steady state of ionomer swelling in the catalyst layer has been reached.

It appears that Ru oxides at the catalyst surface can be reduced continuously during cell conditioning. The near constant integrated areas under the CO-stripping peaks and broadened CO-stripping shapes indicate that the number of Pt/Ru bimetallic alloy surface sites does not vary, but the surface composition distribution broadens.

Heat-treatment can have a major impact on the characteristics of anodes in DMFCs, since heat-treatment influences the ionomer crystallinity and hence affects its swelling behavior. The 40-min-cured anode with low ionomer crystallinity swells more during cell conditiong and creates a much denser anode structure, thus giving rise to higher MeOH crossover resistance and different anode polarization characteristics when compared with the 60-min-cured anode. Various characterization data and our analysis suggest that heat treatment influences primarily the transport properties of the anode, while the interfacial properties between the catalyst and ionomer, i.e. on the triple-phase boundary, remain unaltered. Future work is needed to further assess the implication of heat treatment on the anode long-term performance as the present results are concerned with beginning-of-the-life behaviors only.

During cell conditioning, the enhanced kinetics of MeOH electrochemical oxidation and severe limiting current phenomena are due to the combination of variation in time-dependent interfacial properties and swelling behavior of ionomer in the anode catalyst layer.

Acknowledgement

Support for this work by DARPA Microsystem Technology Office (MTO) under grant no. DAAH01-1-R001 is gratefully acknowledged.

References

[1] A.S. Aricò, S. Srinivasan, V. Antonucci, Fuel Cells 1 (2001) 133.
[2] S.S. Kocha, in: W. Vielstich, A. Lamm, H. Gasteiger (Eds.), Handbook of Fuel Cells–Fundamentals Technology and Applications, vol. 3, Wiley, 2003 (Chapter 43).
[3] M.S. Wilson, S. Gottesfeld, J. Appl. Electrochem. 22 (1992) 1.
[4] M.S. Wilson, J.A. Valerio, S. Gottesfeld, Electrochim. Acta 40 (1995) 355.
[5] M.S. Wilson, S. Gottesfeld, J. Electrochem. Soc. 139 (1992) 28.
[6] M.S. Wilson, US Patent 5,211,984 (1993).
[7] M.S. Wilson, US Patent 5,234,777 (1993).
[8] M. Uchida, Y. Fukuoka, Y. Sugawara, H. Ohara, A. Ohta, J. Electrochem. Soc. 145 (1998) 3708.
[9] M. Uchida, Y. Aoyama, N. Eda, A. Ohta, J. Electrochem. Soc. 142 (1995) 463.
[10] M. Uchida, Y. Aoyama, N. Eda, A. Ohta, J. Electrochem. Soc. 142 (1995) 4143.
[11] T.-Y. Yang, Y.-G. Yoon, G.-G. Park, W.-Y. Lee, C.-S. Kim, J. Power Sources 127 (2003) 230.
[12] G. Bender, T.A. Zawodzinski, A.P. Saab, J. Power Sources 124 (2003) 114.
[13] A.S. Aricò, P. Creti, P.L. Antonucci, J. Cho, H. Kim, V. Antonucci, Electrochim. Acta 43 (1998) 3719.
[14] S.J. Lee, S. Mukerjee, J. McBreen, Y.W. Rho, Y.T. Kho, T.H. Lee, Electrochim. Acta 43 (1998) 3693.
[15] E. Passalacqua, F. Lufrano, G. Squadrito, A. Patti, L. Giorgi, Electrochim. Acta 46 (2001) 799.
[16] C. Lim, C.Y. Wang, J. Power Sources 113 (2003) 145.
[17] G.Q. Lu, C.Y. Wang, T.J. Yen, X. Zhang, Electrochim. Acta 49 (2004) 821.
[18] M. Watanabe, M. Tomikawa, A. Motoo, J. Electroanal. Chem. 195 (1985) 81.
[19] C. Boyer, S. Gamburzev, O. Velve, S. Srinivasan, A.J. Appleby, Electrochim. Acta 43 (1998) 3703.
[20] A.P. Saab, F.H. Garzon, T.A. Zawodzinski, J. Electrochem. Soc. 149 (2002) A1541.
[21] M.C. Lefebvre, R.B. Martin, P.G. Pickup, Electrochem, Solid State Lett. 140 (1999) 259.
[22] M. Murth, 202nd Electrochemical Society Meeting, Salt Lake City, UT, 20–24, October 2002.
[23] S. Ha, C.A. Rice, R.I. Masel, A. Wiechowski, J. Power Sources 112 (2002) 665.
[24] H.N. Dinh, X. Ren, F.H. Garzon, P. Zelenay, S. Gottesfeld, J. Electroanal. Chem. 491 (2000) 222.
[25] W.S. Li, L.P. Tian, Q.M. Huang, H. Li, H.Y. Chen, X.P. Lian, J. Power Sources 104 (2002) 281.

[26] S. lj Gojković, T.R. Vidaković, D.R. Đurović, Electrochim. Acta 48 (2003) 3607.
[27] X. Ren, T.E. Springer, S. Gottesfeld, J. Electrochem. Soc. 147 (2000) 92.
[28] A.L. Rollet, G. Gebel, J.P. Simonin, P. Turq, J. Polym. Sci.: Part B: Polym. Phys. 39 (2001) 548.
[29] R.B. Moore III, C.R. Martin, Macromolecules 21 (1988) 1334.
[30] G. Gebel, P. Aldebert, M. Pineri, Macromolecules 20 (1987) 1425.
[31] R.S. Yeo, J. Appl. Polym. Sci. 32 (1986) 5733.
[32] G. Gebel, P. Aldebert, M. Pineri, Polymer 34 (1993) 333.
[33] F.Q. Liu, B.Y. Yi, D.M. Xing, J.Y. Yu, H.M. Zhang, J. Membr. Sci. 212 (2003) 213.
[34] G.Q. Lu, C.Y. Wang, in: B. Sunden, M. Fahgri (Eds.), Transport Phenomena in Fuel Cells, WIT Press, 2004 (in press).